

Coupled-channel analysis of $K\Lambda$ production in the nucleon resonance regionV. Shklyar,^{†,‡} H. Lenseke, and U. Mosel*Institut für Theoretische Physik, Universität Giessen, D-35392 Giessen, Germany*

(Received 4 May 2005; published 29 July 2005)

A unitary coupled-channel effective Lagrangian model is applied to the combined analysis of the $(\pi, \gamma)N \rightarrow K\Lambda$ reactions in the energy region up to 2 GeV. To constrain the resonance couplings to the $K\Lambda$ final state the recent photoproduction data obtained by the SAPHIR, Spring-8, and CLAS groups are included in the calculations. The main resonance contributions to the process stem from the $S_{11}(1650)$, $P_{13}(1720)$, and $P_{13}(1900)$ states. The second peak at 1.9 GeV seen in the photoproduction cross-section data is described as a coherent sum of the resonance and background contributions. The prediction for the beam polarization observable is presented.

DOI: [10.1103/PhysRevC.72.015210](https://doi.org/10.1103/PhysRevC.72.015210)

PACS number(s): 14.20.Gk, 11.80.-m, 13.75.Gx, 13.30.Eg

I. INTRODUCTION

The associated strangeness production provides a very interesting tool for investigations of the nucleon resonance spectrum. Although previous experimental studies of the $\pi N \rightarrow K\Lambda$ reactions were hampered by poor statistics, recently interest in associated strangeness production has been rekindled by the new photoproduction data from SAPHIR, CLAS, and Spring-8. One of the motivations of those studies was a search for the “missing” resonances that might be weakly coupled to the πN final state [1] and therefore are not seen in πN scattering.

The assumption that such “hidden” resonances can be excited in photon-induced reactions led to the experimental study of $K\Lambda$ and $K\Sigma$ photoproduction with the high-resolution SAPHIR spectrometer at Bonn. The first results published in 1998 [2] revealed a resonance-like structure in the total $\gamma N \rightarrow K\Lambda$ cross section at 1.9 GeV. This behavior was explained by Penner and Mosel [3] as an interference pattern between the nucleon and t -channel background contributions whereas Mart and Bennhold [4] identified it with a resonance contribution from the “missing” $D_{13}(1960)$ state. In a recent coupled-channel study of the associated strangeness production [5] a contribution from the third S_{11} resonance state is found to be necessary to describe the CLAS data [6].

Numerous other models have been developed to describe the $K\Lambda$ data and extract the resonance couplings to these channels. Most models are based on the single-channel formulation of the scattering problem. They mainly differ in their treatment of the background contributions and number of the resonances included [4,7–9]. In addition, Coupled-channel models [3,5,10–14] have also been developed to simultaneously describe the pion- and photon-induced reactions. These approaches are advantageous since the threshold and rescattering effects in the intermediate channels are also taken into account. The importance of a coupled-channel description

of the $K\Lambda$ photoproduction has been demonstrated in [12]. It has been shown that the contribution of the intermediate πN channel to the total $\gamma N \rightarrow K\Lambda$ cross section can be up to 20%.

Despite the extensive studies of $K\Lambda$ photoproduction the situation is far from satisfactory. Almost all models demonstrate a good agreement with the experimental data but predict different resonance contributions to the process. The problems in the interpretation of the associated strangeness photoproduction data in the nucleon resonance region are well documented [8,9,15]. Therefore, the central question of the resonance contribution to the $K\Lambda$ channel is still open. Keeping that in mind, we have performed a new study of the pion- and photon-induced reactions within the unitary coupled-channel effective Lagrangian approach developed in [3,10,11,16].

Our results for the nonstrange channels and resonance parameters extracted are presented in [17]. In this paper we continue the discussion started in [17], focusing on the results on the $K\Lambda$ production in the pion- and photon-nucleon scattering. First, in contrast to our previous calculations [3,11] the model space has been extended to include the contributions from the spin- $\frac{5}{2}$ resonances [10,17]. Although the effect of these states on $\pi N \rightarrow K\Lambda$ reactions is found to be small their contributions to photoproduction might be enhanced. Second, new experimental data from the CLAS [6], Spring-8 [18], and SAPHIR [19] collaborations have become available. This raises the question of whether these data can be described by already known mechanisms [3,11,17] or require further investigations of the $K\Lambda$ reaction mechanism.

Since the polarization observables are found to be extremely useful to distinguish among various model assumptions on the $\gamma N \rightarrow K\Lambda$ reaction [9], we predict polarization observables that can be measured at the present experimental facilities. This study becomes especially interesting in light of the prospect of future high-resolution data from CLAS and Spring-8.

We start in Sec. II with a short review of the progress made in studying $K\Lambda$ photoproduction. The main ingredients of the applied model are discussed in Sec. III. The database and details of the calculations are presented in Sec. IV. In Sec. V we discuss the obtained results and finish with a summary.

[†]On leave from Far Eastern State University, RU-690600 Vladivostok, Russia.

[‡]Electronic address: shklyar@theo.physik.uni-giessen.de

II. OVERVIEW OF THE $K\Lambda$ PHOTOPRODUCTION

Extensive studies of the $K\Lambda$ photoproduction are made in [8,9,20,21] utilizing a tree-level description of the transition amplitude. In their latest work [9] Ireland, Janssen, and Ryckebusch attempted to distinguish among different resonance contributions to the $K\Lambda$ channel by using a generic algorithm analysis. Based on this procedure, these authors conclude that a $P_{11}(1900)$ state is the most favorable candidate for the resonant contribution to the $K\Lambda$ photoproduction apparently seen at 1.9 GeV. The contribution from the S_{11} and D_{13} states is only weakly supported but, nevertheless, cannot be excluded in these calculations.

Guided by the results of quark model predictions of Capstic and Roberts [1], Mart *et al.* performed an analysis [7] of the recent photoproduction data from the SAPHIR collaboration [19]. This approach uses a Breit-Wigner (BW) parametrization of the resonance amplitudes and, therefore, is similar to that of [8,9,20,21]. The calculations of [7] suggest a large number of new (hidden) resonances that can contribute to the process.

The main shortcoming of the single-channel BW models is that the rescattering effects are missed in such parametrizations. If one assumes a resonance that couples strongly to the $K\Lambda$ final state, the corresponding part of its width should be accounted for by rescattering in the intermediate $K\Lambda$ channel. Therefore, the BW parametrization of resonance contributions brings an ambiguity into the calculations. This point has been explicitly demonstrated in the work of Usov and Scholten [14] with the example of the $S_{11}(1650)$ resonance. In the tree-level approximation to the $K\Lambda$ photoproduction amplitude the contribution from this resonance is proportional to the product of two coupling constants: $g_{\gamma NN^*} g_{K\Lambda N^*}$. In contrast, as soon as rescattering effects are taken into account the final result is found to be extremely sensitive to the value of $g_{K\Lambda N^*}$ alone, even if the common strength $g_{\gamma NN^*} g_{K\Lambda N^*}$ is kept constant. Therefore, the conclusions on the resonance couplings to the $K\Lambda$ final state are different from those from the BW calculations.

In other words, unitarity should be maintained in any calculations aimed at extracting information on the resonance contributions to the $K\Lambda$ channel from experiment. Recently, models that preserve unitarity have been applied to the analysis of the $K\Lambda$ production in the pion- and photon-induced reactions [3,5,11,13,14,22–24]. In the effective Lagrangian approach of Lutz *et al.* [13] pointlike vertices are used to describe meson-nucleon interactions, enforcing both unitarity and analyticity. However, the assumption made about the S - and D -wave dominance of the reaction mechanism limits these calculations to energies close to the reaction threshold.

Another interesting coupled-channel approach satisfying unitarity and analyticity is developed in [5,12,24]. In this model the rescattering effects in the intermediate πN channel are taken into account. This is achieved by using πN amplitudes from the SAID group analysis [25]. In [5] the authors find a strong need for a $S_{11}(1900)$ resonance contribution to the $K\Lambda$ photoproduction to describe the CLAS data at 1.9 GeV. Concluding on the importance of the πN rescattering process the authors, however, do not check whether other inelastic channels are affecting the results of their calculations.

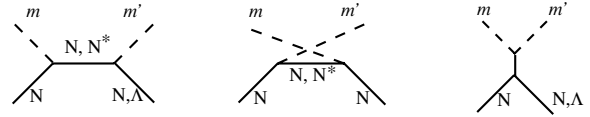


FIG. 1. s -, u -, and t -channel contributions to the interaction potential. m and m' stand for, respectively, initial and final $\pi, \gamma, \omega, K, \dots$ etc.

Recently, Usov and Scholten [14] presented a coupled-channel model for the pion- and photon-induced reactions with $\pi N, \eta N, K\Lambda$, and $K\Sigma$ in the final state. This approach is based on the K -matrix formalism and is thus similar to the Giessen model [3,10,11,16,17,22,23] to be discussed in the following. To constrain the resonance contributions to the $K\Lambda$ final state, πN elastic and photoproduction data were also described with satisfactory agreement. The main result of [14] is that the $K\Lambda$ photoproduction above 1.7 GeV is strongly influenced by background contributions. As we will see later, our present calculations in general support the conclusions drawn in [14].

III. GIESSEN MODEL

The details of the model, interaction Lagrangians, and results for the nonstrange channels can be found in [3,11] and [17], respectively. Here, we only briefly outline the main ingredients of our model.

The Bethe-Salpeter equation (BSE) is solved in the K -matrix approximations to calculate the scattering amplitudes of different reactions [3,11,16]. The validity of this approximation is discussed in [11,17]. The interaction potential (K matrix) in the BSE is constructed as a sum of the s -, u -, and t -channel tree-level Feynman diagrams contributions, depicted in Fig. 1, and calculated from the corresponding effective interaction Lagrangians. After the partial wave decomposition [3,11,16] the BSE reduces to the following set of algebraic equations for the scattering T matrix:

$$T_{fi}^{J\pm, I} = \left[\frac{K^{J\pm, I}}{1 - iK^{J\pm, I}} \right]_{fi}, \quad (1)$$

where $J\pm, I$ are total spin, parity, and isospin of the initial and final states $f, i = \pi N, K\Lambda$, etc.

The resonance couplings to $K\Lambda$ are given in [3,10,11,17]. Each meson and baryon vertex is dressed by a corresponding form factor, which according to [11] is chosen as

$$F_p(q^2, m^2) = \frac{\Lambda^4}{\Lambda^4 + (q^2 - m^2)^2}, \quad (2)$$

thereby cutting off large 4-momenta $q^2 \gg \Lambda^2$.

To reduce the number of free parameters we use the same cutoffs for all resonances with given spin J (see [17]); for example, $\Lambda_i^{N^*(1535)} = \Lambda_j^{N^*(1650)}$, where indices i, j run over all final states $i, j = \pi N, \eta N, K\Lambda, \dots$ etc. Also, we identify the cutoff at the $NK\Lambda$ vertex with the nucleon cutoff: $\Lambda_{NK\Lambda} = \Lambda_N = 0.95$ GeV.

The nonresonant part of the transition amplitude $(\pi, \gamma)N \rightarrow K\Lambda$ is similar to the one used in [3,11,17] and

consists of the nucleon Born term and t -channel contributions with the K^* , K_0^* , and K_1 mesons in the intermediate state. Taking the values for the decay widths from PDG [26], we extract the following coupling constants:

$$\begin{aligned} g_{K^*K\pi} &= -6.500, & g_{K_0^*K\pi} &= -0.900, \\ g_{K^{*+}K^+\gamma} &= -0.414, & g_{K^{*0}K^0\gamma} &= 0.631, \\ g_{K_1^+K^+\gamma} &= 0.217, & g_{K_1^0K^0\gamma} &= 0.217. \end{aligned} \quad (3)$$

Note that we use the same $\Lambda_t = 0.75$ GeV at the corresponding t -channel vertices for both associated strangeness production and nonstrange channels [17]. As in our previous studies [3,11] we do not include the u -channel diagrams in the $(\pi, \gamma)N \rightarrow K\Lambda$ reaction. The calculation of such contributions would require knowledge of a priori unknown couplings to the intermediate strange baryons. To keep the model as simple as possible, these diagrams are not taken into account here.

IV. DETAILS OF THE CALCULATIONS

Our previous calculations on associated strangeness production [3,10,11] were based on the experimental data published before 2002 (see also [16] for details). Since then a new set of photoproduction data has become available. This includes the photon beam asymmetry obtained by Spring-8 [18], and the differential cross sections and the polarization of the outgoing Λ from SAPHIR [19] and CLAS [6]. Therefore, in the $\gamma N \rightarrow K\Lambda$ channel we no longer use the previous SAPHIR data [2] but incorporate all recent measurements [6,18,19] for energies $\sqrt{s} \leq 2$ GeV into our database.

Comparing the $\gamma N \rightarrow K\Lambda$ differential cross sections independently measured by SAPHIR [19] and CLAS [6] one finds a significant disagreement between the two data sets near 1.9 GeV. To avoid this problem, in a first step we include in the fit only those data that coincide, within their error bars, with each other. Using this truncated database, a full coupled-channel calculations on the $\pi N \rightarrow \pi N, 2\pi N, \eta N, \omega N, K\Lambda, K\Sigma$ and $\gamma N \rightarrow \gamma N, \pi N, \eta N, \omega N, K\Lambda, K\Sigma$ reactions has been carried out. The results of this calculations have been presented in [17], which focuses on the description of the non-strange channels. To pin down the $K\Lambda$ production mechanism further, we constructed two different sets of parameters. Set $S(C)$ corresponds to the solution obtained with the differential $\gamma N \rightarrow K\Lambda$ cross section data exclusively from the SAPHIR [19] (CLAS [6]) measurements.

At this step we allow all couplings to the $K\Lambda$ final state to be varied during the fit. Other parameters of the model that correspond to the couplings to the nonstrange final states ($\gamma N, \pi N$, etc.; see [17]) have been held fixed at this stage.

Finally, we obtain two solutions S and C that differ in their treatment of the $K\Lambda$ channel. As will be seen later, the main difference between these two solutions lies in the different description of the background contributions to the $K\Lambda$ photoproduction. As a result, the additional constraint from the SAPHIR or CLAS data hardly affects the nonstrange channels. Thus, the deviation from the χ^2 obtained in [17] for the $\pi N, 2\pi, \omega N$, etc. does not exceed 1.5%.

TABLE I. Branching decay ratios of nucleon resonances into the $K\Lambda$ final state extracted in the calculations with C and S parameter sets, respectively. The sign of the corresponding coupling constant is shown in brackets (all πN couplings are chosen to be positive; see [17]). In the last column the summary results for resonances with masses above the $K\Lambda$ threshold are given. The corresponding errors are shown in brackets. The resonance mass is given in MeV; the decay ratios are in percent.

$L_{2I,2S}$	Mass ^a	$R_{K\Lambda}(C)$	$R_{K\Lambda}(S)$	$\bar{R}_{K\Lambda}$
$S_{11}(1535)$	1526	1.3 ^b	1.26 ^b	
$S_{11}(1650)$	1664	3.2(+)	4.6(+)	4(1)
$P_{11}(1440)$	1517	1.48 ^b	-0.71 ^b	
$P_{11}(1710)$	1723	6.8(+)	3.1(+)	5(3)
$P_{13}(1720)$	1700	4.6(+)	4.0(+)	4.3(0.4)
$P_{13}(1900)$	1998	2.4(+)	2.3(+)	2.4(0.3)
$D_{13}(1520)$	1505	-0.58 ^b	-0.33 ^b	
$D_{13}(1950)$	1934	0.1(+)	0.1(-)	0.1(0.1)
$D_{15}(1675)$	1666	0.2(+)	0.1(+)	0.1(0.1)
$F_{15}(1680)$	1676	0.0(+)	0.0(+)	0.1(0.1)
$F_{15}(2000)$	1946	0.0(+)	0.2(-)	0.1(0.1)

^aFixed in the previous calculations [17].

^bThe coupling is given since the resonance mass is below the threshold.

In the present study we obtain for the $K\Lambda$ photoproduction process $\chi^2_{K\Lambda} = 2.0$ (2.2) in the $S(C)$ calculation. Note that a comparison of these values with the results of the previous calculations [3] should be taken with care since the present study uses different experimental input.

The couplings that have been varied in the fit are presented in Tables I and II. All other model parameters can be found in [17].

V. RESULTS AND DISCUSSION

Since the recent $K\Lambda$ photoproduction data [6,19] give an indication for “missing” resonance contributions, a combined analysis of the $(\pi, \gamma)N \rightarrow K\Lambda$ reactions becomes inevitable to pin down these states. Assuming small couplings to πN , these “hidden” states should not exhibit themselves in the pion-induced reactions and, consequently, in the $\pi N \rightarrow K\Lambda$ reaction. The aim of the present calculations is to explore to what extent the new data can be explained by known reaction mechanisms [3], without introducing new resonances.

The obtained nucleon resonance properties are presented in Table I. The decay ratios to the nonstrange final states and the electromagnetic properties can be found in [17]. We did not aim to distinguish between the CLAS and SAPHIR data in the present calculations. Performing different calculations we

TABLE II. Nucleon and t -channel couplings. First line lists C calculations; second line lists S calculations (see text).

g	Value	g	Value	g	Value	g	Value
$g_{N\Lambda K}$	-6.04	$g_{N\Lambda K_0^*}$	32.2	$g_{N\Lambda K^*}$	2.28	$\kappa_{N\Lambda K^*}$	-0.01
	-4.70		32.5		7.00		-0.06

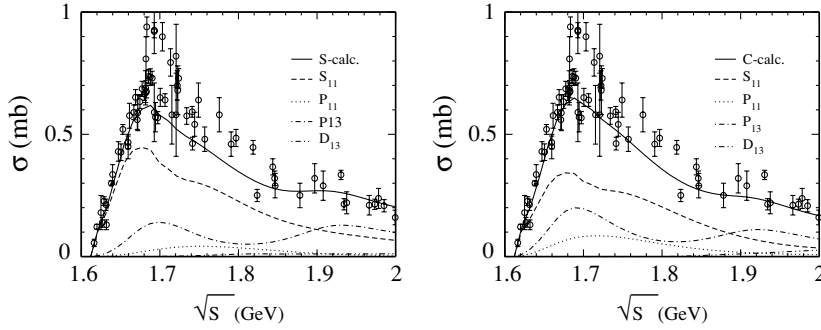


FIG. 2. $\pi^- p \rightarrow K^0 \Lambda$ total cross section. Partial wave cross sections calculated using set S (left) and set C (right). Experimental data are taken from [27–29].

only test the sensitivity of the extracted resonance parameters to the various experimental input.

A. $\pi N \rightarrow K \Lambda$

We corroborate our previous findings [11] where the major contributions to this reaction are found to be from the S_{11} and P_{13} partial waves (see Fig. 2). However, in contrast to the results in [11] the role of the S_{11} partial wave becomes more pronounced in the present calculations. Both S and C calculations give a similar description of $\pi N \rightarrow K \Lambda$. The peaking behavior observed in the S_{11} partial wave near 1.67 GeV is induced by the $S_{11}(1650)$ resonance. The P_{13} wave consists of the $P_{13}(1720)$ and $P_{13}(1900)$ resonance contributions, which develop the two peaks at 1.7 and 1.95 GeV, respectively.

Because of the aforementioned partial disagreement between the CLAS and SAPHIR photoproduction data, the S and C calculations differ in their description of the nonresonance couplings to $K \Lambda$. This leads to different background strengths for the S_{11} , P_{11} , and P_{13} partial waves, leaving, however, the $P_{13}(1720)$ and $P_{13}(1900)$ resonance couplings almost unchanged (see Table I). Comparing the S and C parameter sets, one sees that the largest difference in the resonance

parameters is observed for the $P_{11}(1710)$ state. However, in the present calculations this resonance is found to be almost completely of inelastic origin with a small branching ratio to πN [17]. Therefore, this state gives only a minor contribution to the reaction and the observed difference in the P_{11} partial wave between S and C results is due to the Born term and the t -channel exchange contributions.

Because the $S_{11}(1650)$ resonance dominates the reaction mechanism near the threshold, the difference in the nonresonance part of the reaction also affects the properties of this state by decreasing the relative decay width $R_{K\Lambda}(1650)$ to the value 3.6 in the C calculations. We do not see any significant effect from the $D_{13}(1985)$ state. This resonance is included in the present calculations, but its couplings to the $K \Lambda$ final state is found to be small (see Table I).

The calculated differential cross sections corresponding to the S - and C -coupling sets are shown in Fig. 3. Both results show good agreement with the experimental data throughout the entire energy region. A difference between the two solutions is only found at forward and backward scattering angles. This is because the CLAS photoproduction cross sections rise at backward angles, an effect not observed by the SAPHIR group (see the discussion to follow). At other scattering angles the S and C results are very similar. The

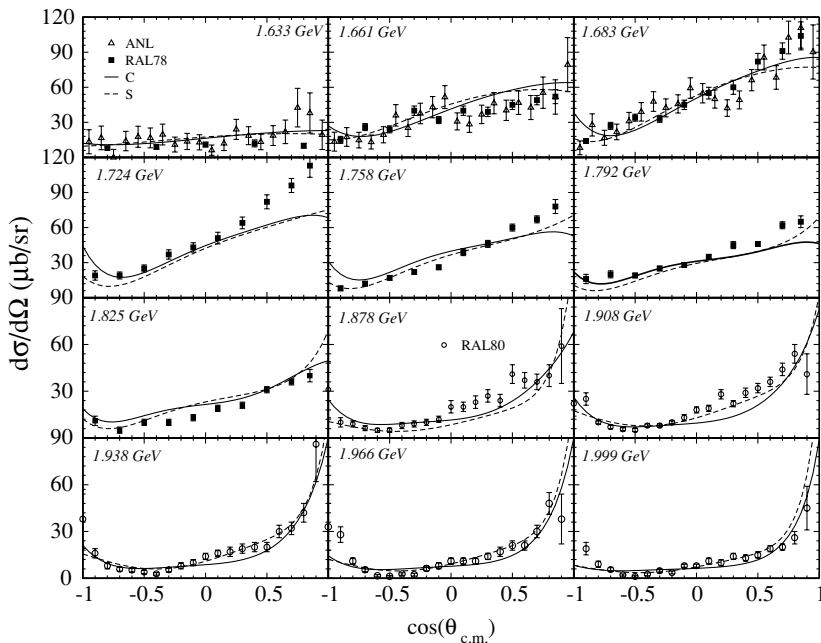


FIG. 3. Comparison of the $\pi N \rightarrow K \Lambda$ differential cross section calculated using the C (solid line) and S (dashed line) sets. Data are taken from RAL78 [27], RAL80 [28], and ANL [29].

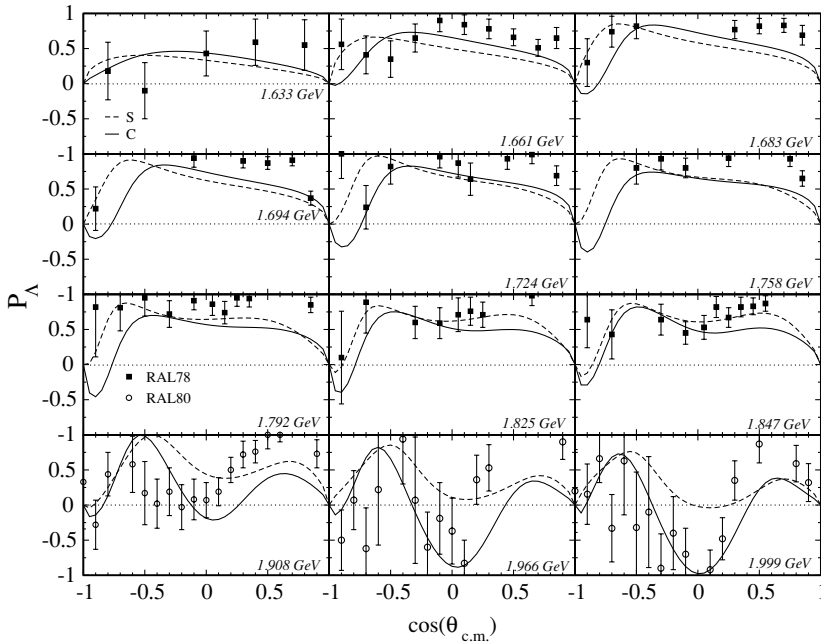


FIG. 4. Comparison of Λ polarization in the $\pi^-p \rightarrow K^0\Lambda$ reaction calculated for two different parameter sets. Data are taken from RAL78 [27] and RAL80 [28].

differences between S and C calculations are more pronounced for the Λ polarization shown in Fig. 4. Again, the main effect is seen at the backward angles where the polarization changes its sign in the C calculations. Unfortunately, the quality of the data does not allow us to pin down the reaction mechanism further.

B. $\gamma N \rightarrow K\Lambda$

The measurement of this reaction performed by Tran *et al.* [2] shows a resonance-like peak in the total photoproduction cross section around 1.9 GeV. The new data published by the SAPHIR [19] and CLAS [6] groups confirm the previous

findings of [2]. Moreover, because of the higher resolution, the peaking behavior in the differential cross sections at 1.9 GeV has been found also for backward scattering angles. The interpretation of these data is controversial in the literature. The main question under discussion is whether in these measurements contributions from presently unknown resonances are observed or if they can be explained by already established reaction mechanisms.

Since our previous investigations of the $K\Lambda$ photoproduction [3] were based on the Tran *et al.* [2] data, those calculations lose the agreement with the new data at 1.9 GeV for the backward scattering angles. Guided by the results of [3] we have performed a new coupled-channel study of this reaction

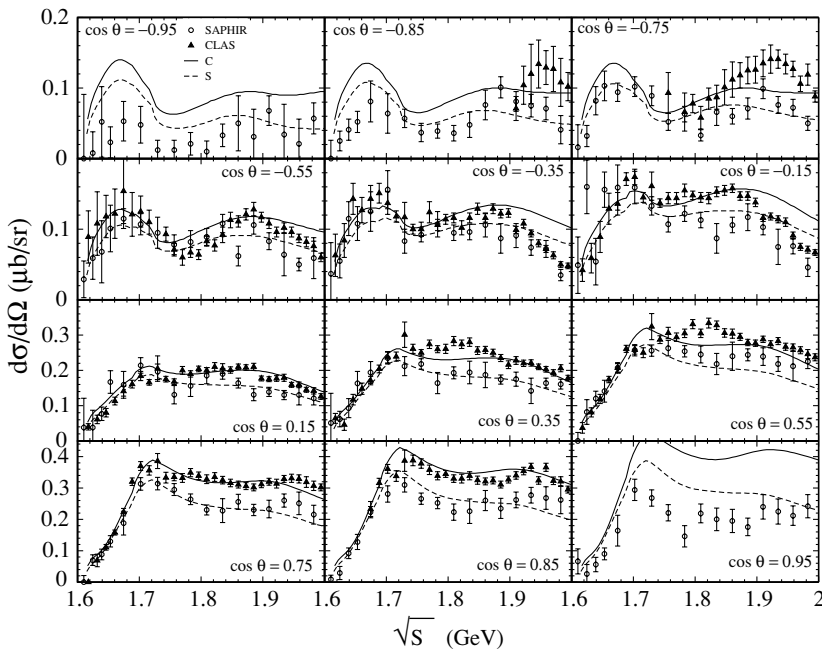


FIG. 5. Comparison of the differential cross sections for the reaction $\gamma p \rightarrow K^+\Lambda$ calculated using C and S parameter sets. Experimental data are taken from [6] (CLAS) and [19] (SAPHIR).

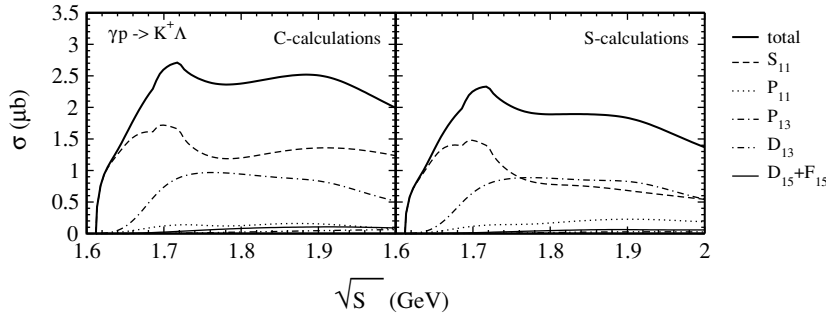


FIG. 6. Partial wave contributions to the total $K\Lambda$ photoproduction cross section.

using separately the CLAS and SAPHIR measurements as two independent input sets (see Sec. IV). The main difference between the CLAS and SAPHIR data is seen at backward and forward directions (Fig. 5). Both measurements show two peaks but disagree in the absolute values of the corresponding differential cross sections. Also, the second peak in the CLAS data is shifted to the lower energy 1.8-GeV peak for scattering angles corresponding to $\cos\theta = 0.35$ and $\cos\theta = 0.55$.

Both the S and C calculations demonstrate good agreement with the corresponding experimental data, although the S calculations lead to a smaller value of $\chi^2_{K\Lambda}$. However, this is not because the measurements of [19] are more consistent with $\pi N \rightarrow K\Lambda$ data. Instead it is because the location of the second peak in the CLAS data changes with scattering angles. Since our differential cross section does not follow the CLAS data at 1.8 GeV and $\cos\theta = 0.35$ and $\cos\theta = 0.55$ (see Fig. 5) the total $\chi^2_{K\Lambda}$ turns out to be larger in the C calculations. Note that if the behavior observed by the CLAS group should be confirmed in future experiments, further assumptions on the reaction mechanism would be required.

Similar to $\pi N \rightarrow K\Lambda$ the major difference between the S and C solutions is the treatment of the nonresonant contributions. Thus, both calculations show two peaks in the differential cross sections at 1.7 and 1.9 GeV. The first peak at 1.67 GeV in both calculations is produced by the $S_{11}(1650)$ resonance (see Fig. 6). The relative contributions to the second peak at 1.9 GeV are different in the C and S solutions. In the C

calculations this structure is described by the S_{11} partial wave. Note that we do not include a third S_{11} resonance with a mass of about 2 GeV as done in [5]. Therefore, the contributions to the S_{11} at higher energies are dominated by the nonresonant reaction mechanisms. The P_{13} partial wave is entirely driven by the $P_{13}(1720)$ and $P_{13}(1900)$ resonance contributions. Switching off these resonance couplings to $K\Lambda$ leads to an almost vanishing P_{13} partial wave. In the S calculations no peaking behavior is found in the S_{11} partial wave at 1.95 GeV. However, the nonresonant effects in the S_{11} channel are still important. The role of the P_{13} resonances is slightly enhanced in the S calculations. The effect from the $P_{11}(1710)$ resonance is found to be small in both calculations owing to destructive interference with the background process. There are no significant contributions from the spin- $\frac{5}{2}$ resonances to the $\gamma N \rightarrow K\Lambda$ reaction. Also, no effect is seen from the $D_{13}(1950)$ resonance.

The calculated photon beam asymmetry Σ_x and recoil polarization P_Λ are shown in Figs. 7 and 8, respectively. Since the beam asymmetry data [18] from the Spring-8 collaboration are available only for energies above 1.94 GeV, these measurements give an insignificant constraint on the model parameters. Therefore, the results for the asymmetry might be regarded as a prediction rather than an outcome of the fit. More information comes from the Λ -polarization data. A good description of the Σ_x and P_Λ data is possible in both the C and S calculations. One can conclude that despite

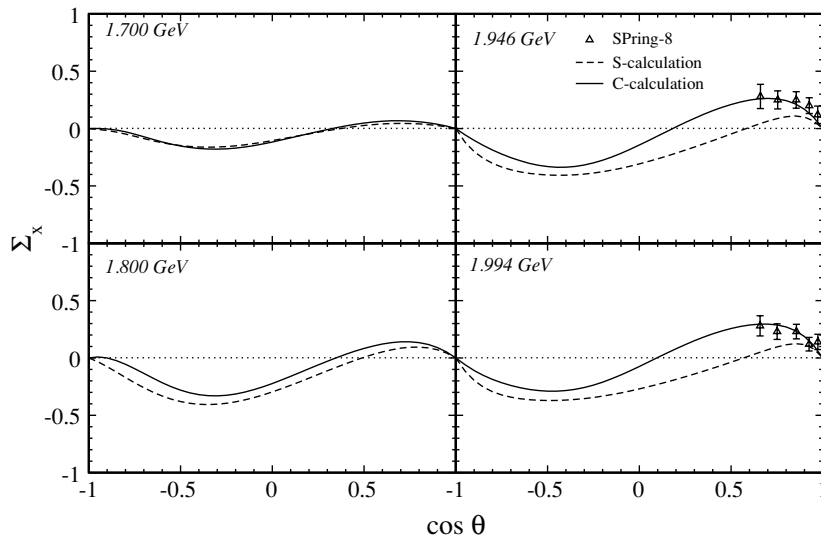


FIG. 7. The calculated photon beam asymmetry. Data are taken from [18].

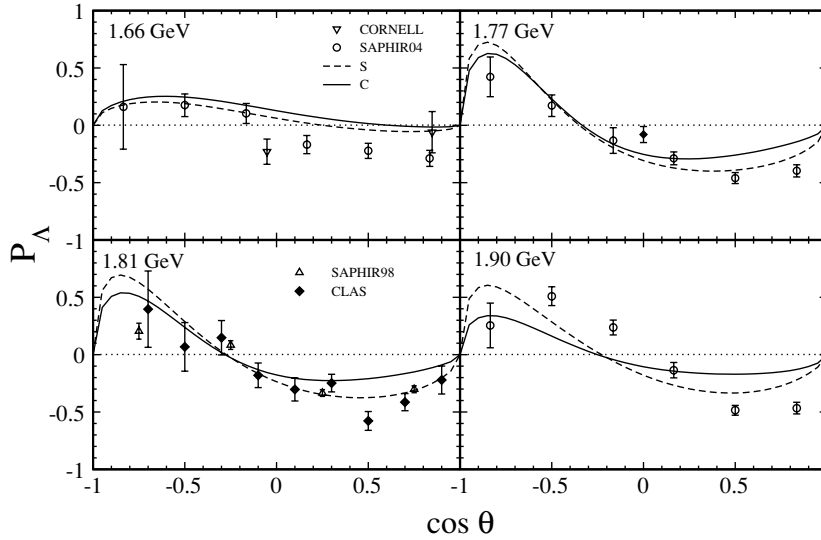


FIG. 8. Λ polarization in the $\gamma p \rightarrow K^+ \Lambda$ reaction. Data are from SAPHIR98 [2], SAPHIR04 [19], CLAS [6], and CORNELL [30].

the differences in the differential cross sections between the data [6,19] the calculated Σ_x and P_Λ observables are very similar in both cases and the main difference between the S and C calculations lies in the background contributions. This also explains why the resonance parameters extracted are fairly insensitive to the parameter set used (see Table I).

VI. SUMMARY

In summary, we have performed a coupled-channel analysis of the $(\pi, \gamma)N \rightarrow K\Lambda$ reaction to extract the nonstrange resonance couplings to the $K\Lambda$ final state. To distinguish the different $K\Lambda$ photoproduction measurements we obtained two independent solutions to the SAPHIR and CLAS data for energies $\sqrt{s} \leq 2$ GeV. The main resonance contributions to the reaction stem from the $S_{11}(1650)$, $P_{13}(1720)$, and $P_{13}(1900)$ states. It is shown that the extracted resonance parameters are hardly sensitive to the observed discrepancy between the different data sets. We have discussed that this is because the differences between the two data sets stem mainly from different nonresonant background contributions.

We do not see any significant effects from the $P_{11}(1710)$ and $D_{13}(1890)$ states. Also, the contributions from the spin- $\frac{5}{2}$ resonances are found to be small. In our coupled-channel approach the second peak in the differential cross section data at 1.9 GeV observed by the SAPHIR and CLAS groups is produced by a coherent sum of the resonance and background contributions, without any evidence for a “missing” resonance. As a test for our model calculations we predict the beam asymmetry to change its sign for moderate angles. This effect can be easily checked at the running experimental facilities such as JLAB and LEPS.

We have checked whether there is room left for further improvement of the agreement of the calculated observables with the $(\pi, \gamma)N \rightarrow K\Lambda$ data. However, before such a new analysis is meaningful the inconsistency between the two data sets has to be resolved.

ACKNOWLEDGMENTS

The work has been supported by Forschungszentrum Juelich.

-
- [1] S. Capstick and W. Roberts, Phys. Rev. D **58**, 074011 (1998).
 - [2] M. Q. Tran *et al.* (SAPHIR), Phys. Lett. **B445**, 20 (1998).
 - [3] G. Penner and U. Mosel, Phys. Rev. C **66**, 055212 (2002).
 - [4] T. Mart and C. Bennhold, Phys. Rev. C **61**, 012201(R) (2000).
 - [5] B. Julia-Diaz, B. Saghai, F. Tabakin, W.-T. Chiang, T.-S. H. Lee, and Z. Li, Nucl. Phys. **A755**, 463 (2005).
 - [6] J. W. C. McNabb *et al.* (The CLAS Collaboration), Phys. Rev. C **69**, 042201(R) (2004).
 - [7] T. Mart, A. Sulaksono, and C. Bennhold, Invited talk at International Symposium on Electrophoto Production of Strangeness on Nucleons and Nuclei (SENDAI 03), Sendai, Japan, 16–18 June, 2003; nucl-th/0411035.
 - [8] S. Janssen, J. Ryckebusch, D. Debruyne, and T. Van Cauteren, Phys. Rev. C **65**, 015201 (2002).
 - [9] D. G. Ireland, S. Janssen, and J. Ryckebusch, Nucl. Phys. **A740**, 147 (2004).
 - [10] V. Shklyar, G. Penner, and U. Mosel, Eur. Phys. J. **A21**, 445 (2004).
 - [11] G. Penner and U. Mosel, Phys. Rev. C **66**, 055211 (2002).
 - [12] W.-T. Chiang, F. Tabakin, T. S. H. Lee, and B. Saghai, Phys. Lett. **B517**, 101 (2001).
 - [13] M. F. M. Lutz, G. Wolf, and B. Friman, Nucl. Phys. **A706**, 431 (2002).
 - [14] A. Usov and O. Scholten, submitted to Phys. Rev. C, nucl-th/0503013.
 - [15] B. Saghai, Invited talk given at International Symposium on Hadrons and Nuclei, Seoul, February 20–22, (2001).
 - [16] G. Penner, Ph.D. thesis (in English), Universität Giessen, 2002, available via <http://theorie.physik.uni-giessen.de>.
 - [17] V. Shklyar, H. Lenske, U. Mosel, and G. Penner, Phys. Rev. C **71**, 055206 (2005).

- [18] R. G. T. Zegers *et al.* (LEPS), Phys. Rev. Lett. **91**, 092001 (2003).
- [19] K. H. Glander *et al.*, Eur. Phys. J. A **19**, 251 (2004).
- [20] S. Janssen, J. Ryckebusch, W. Van Nespen, D. Debruyne, and T. Van Cauteren, Eur. Phys. J. A **11**, 105 (2001).
- [21] S. Janssen, D. G. Ireland, and J. Ryckebusch, Phys. Lett. **B562**, 51 (2003).
- [22] T. Feuster and U. Mosel, Phys. Rev. C **58**, 457 (1998).
- [23] T. Feuster and U. Mosel, Phys. Rev. C **59**, 460 (1999).
- [24] W.-T. Chiang, B. Saghai, F. Tabakin, and T. S. H. Lee, Phys. Rev. C **69**, 065208 (2004).
- [25] R. A. Arndt, W. J. Briscoe, I. I. Strakovsky, R. L. Workman, and M. M. Pavan, Phys. Rev. C **69**, 035213 (2004).
- [26] K. Hagiwara *et al.* (Particle Data Group), Phys. Rev. D **66**, 010001 (2002).
- [27] R. D. Baker *et al.*, Nucl. Phys. **B141**, 29 (1978).
- [28] D. H. Saxon *et al.*, Nucl. Phys. **B162**, 522 (1980).
- [29] T. M. Knael *et al.*, Phys. Rev. D **11**, 1 (1975).
- [30] H. Thom, E. Gabathuler, E. Jones, B. McDaniel, and W. M. Woodward, Phys. Rev. Lett. **11**, 433 (1963).